NASA/TM–2014-218540
NESC-RP-13-00911

Maximum Expected Wall Heat Flux and Maximum Pressure after Sudden Loss of Vacuum Insulation on the Stratospheric Observatory for Infrared Astronomy (SOFIA) Liquid Helium (LHe) Dewars

Eugene K. Ungar/NESC
Langley Research Center, Hampton, Virginia

October 2014

NASA STI Program . . . in Profile

Since its founding, NASA has been dedicated to the advancement of aeronautics and space science. The NASA scientific and technical information (STI) program plays a key part in helping NASA maintain this important role.

The NASA STI program operates under the auspices of the Agency Chief Information Officer. It collects, organizes, provides for archiving, and disseminates NASA's STI. The NASA STI program provides access to the NASA Aeronautics and Space Database and its public interface, the NASA Technical Report Server, thus providing one of the largest collections of aeronautical and space science STI in the world. Results are published in both non-NASA channels and by NASA in the NASA STI Report Series, which includes the following report types:

- TECHNICAL PUBLICATION. Reports of completed research or a major significant phase of research that present the results of NASA Programs and include extensive data or theoretical analysis. Includes compilations of significant scientific and technical data and information deemed to be of continuing reference value. NASA counterpart of peer-reviewed formal professional papers, but having less stringent limitations on manuscript length and extent of graphic presentations.

- TECHNICAL MEMORANDUM. Scientific and technical findings that are preliminary or of specialized interest, e.g., quick release reports, working papers, and bibliographies that contain minimal annotation. Does not contain extensive analysis.

- CONTRACTOR REPORT. Scientific and technical findings by NASA-sponsored contractors and grantees.

- CONFERENCE PUBLICATION. Collected papers from scientific and technical conferences, symposia, seminars, or other meetings sponsored or co-sponsored by NASA.

- SPECIAL PUBLICATION. Scientific, technical, or historical information from NASA programs, projects, and missions, often concerned with subjects having substantial public interest.

- TECHNICAL TRANSLATION. English-language translations of foreign scientific and technical material pertinent to NASA's mission.

Specialized services also include organizing and publishing research results, distributing specialized research announcements and feeds, providing information desk and personal search support, and enabling data exchange services.

For more information about the NASA STI program, see the following:

- Access the NASA STI program home page at *http://www.sti.nasa.gov*

- E-mail your question to help@sti.nasa.gov

- Fax your question to the NASA STI Information Desk at 443-757-5803

- Phone the NASA STI Information Desk at 443-757-5802

- Write to:
  STI Information Desk
  NASA Center for AeroSpace Information
  7115 Standard Drive
  Hanover, MD 21076-1320

NASA/TM–2014-218540
NESC-RP-13-00911

Maximum Expected Wall Heat Flux and Maximum Pressure after Sudden Loss of Vacuum Insulation on the Stratospheric Observatory for Infrared Astronomy (SOFIA) Liquid Helium (LHe) Dewars

Eugene K. Ungar/NESC
Langley Research Center, Hampton, Virginia

National Aeronautics and
Space Administration

Langley Research Center
Hampton, Virginia 23681-2199

October 2014

Acknowledgments

The author wishes to thank Mr. Andrew Hong (JSC) for performing the numerical analysis for the present work.

The use of trademarks or names of manufacturers in the report is for accurate reporting and does not constitute an official endorsement, either expressed or implied, of such products or manufacturers by the National Aeronautics and Space Administration.

Available from:

NASA Center for AeroSpace Information
7115 Standard Drive
Hanover, MD 21076-1320
443-757-5802

Maximum Expected Wall Heat Flux and Maximum Pressure after Sudden Loss of Vacuum Insulation on the Stratospheric Observatory for Infrared Astronomy (SOFIA) Liquid Helium (LHe) Dewars

August 28, 2014

Report Approval and Revision History

NOTE: This document was approved at the August 28, 2014, NRB. This document was submitted to the NESC Director on September 2, 2014, for configuration control.

Approved:	*Original Signature on File*	9/3/14
	NESC Director	Date

Version	Description of Revision	Office of Primary Responsibility	Effective Date
1.0	Initial Release	Hank Rotter, NASA Technical Fellow for Life Support/Active Thermal, JSC	8/28/14
1.1	Per Stakeholder request, removed the Distribution Limitation statement (U.S. Government Agencies and U.S. Government Agency Contractors Only) to make Publicly Available. (*Director's signature not required*)	Hank Rotter, NASA Technical Fellow for Life Support/Active Thermal, JSC	9/11/14

Table of Contents

List of Figures

List of Tables

Technical Assessment Report

1.0 Notification and Authorization

Mr. William Condzella, NASA Safety and Mission Assurance for the Stratospheric Observatory for Infrared Astronomy (SOFIA) Program at the Armstrong Flight Research Center, requested the NASA Engineering and Safety Office (NESC) evaluate and determine the maximum boil off rate of the cryogenic helium (He) dewar after a sudden loss of vacuum jacket thermal protection and its effect on the dewar pressure.

Dr. Eugene Ungar, Discipline Deputy for the Life Support/Active Thermal Technical Discipline Team at Johnson Space Center (JSC), was selected as the technical lead for this assessment.

The key stakeholder for this assessment is Mr. William Condzella.

2.0 Signature Page

Submitted by:

Team Signature Page on File – 9/4/14

Dr. Eugene K. Ungar   Date

Signatories declare the findings, observations, and NESC recommendations compiled in the report are factually based from data extracted from program/project documents, contractor reports, and open literature, and/or generated from independently conducted tests, analyses, and inspections.

3.0 Team List

Name	Discipline	Organization
Core Team		
Eugene Ungar	NESC Technical Lead, Discipline Deputy for the Life Support/Active Thermal Technical Discipline Team	JSC
Pam Throckmorton	MTSO Program Analyst	LaRC
Administrative Support		
Erin Moran	Technical Writer	LaRC/AMA

3.1 Acknowledgements

The author wishes to thank Mr. Andrew Hong (JSC) for performing the numerical analysis for the present work.

4.0 Executive Summary

The aircraft-based Stratospheric Observatory for Infrared Astronomy (SOFIA) is a platform for multiple infrared observation experiments. The experiments carry sensors cooled to liquid helium (LHe) temperatures. The LHe supply is contained in large (i.e., 10 liters or more) vacuum-insulated dewars. A question arose regarding the heat input and peak pressure that would result from a sudden loss of the dewar vacuum insulation. Air entering the vacuum cavity would condense and freeze, providing a large heat input to the LHe. This would cause the LHe to expand and vaporize resulting in a dramatic increase in the dewar pressure.

Owing to concerns about the adequacy of dewar pressure relief in the event of a sudden loss of the dewar vacuum insulation, the SOFIA Program engaged the NASA Engineering and Safety Center (NESC) to answer three questions:

1. What is the expected wall heat flux into the dewar in the event of a sudden loss of vacuum insulation?
2. What is an appropriate method to calculate the maximum pressure that would occur under the expected heat flux?
3. What wall heat flux can be accommodated by the dewars that have been accepted and are scheduled to fly on the SOFIA?

This report summarizes and assesses the experiments that have been performed to measure the heat flux into LHe dewars following a sudden vacuum insulation failure, describes the physical limits of heat input to the dewar, and provides an NESC recommendation for the wall heat flux that should be used to assess the sudden loss of vacuum insulation case.

This report also assesses the methodology used by the SOFIA Program to predict the maximum pressure that would occur following a loss of vacuum event. It provides an alternate, physically complete methodology that should be used to calculate the effluent mass flux that must be accommodated after a sudden vacuum leak and the accompanying dewar pressure. This revised methodology is recommended for future calculations to predict the peak dewar pressure in the event of a sudden loss of vacuum insulation.

5.0 Problem Description and Experimental Results

Typical SOFIA LHe dewar maximum normal operating pressures range from 175 to 315 kPa (peak pressure), bracketing the He critical pressure of 227.5 kPa. Thus, the behavior of the He under high heat input in both the two-phase and supercritical regions must be understood to adequately design the dewar pressure relief system.

5.1 Wall Heat Flux Following Loss of Vacuum

Experiments

A number of experiments have been performed to measure the LHe dewar heat flux that results from a sudden loss of vacuum insulation.

Lehmann and Zahn [ref. 1] performed careful, well-instrumented loss of vacuum tests on a vented 100-liter LHe dewar with no superinsulation. A fast-opening, 32-millimeter (mm) inner diameter valve on the dewar vacuum port created a sudden loss of vacuum. The complete LHe charge vented within 20 seconds. The He exit flow was largely unrestricted, resulting in a maximum dewar pressure of 133 kPa, well below the He critical pressure. This allowed the mass flow rate of the He exiting the dewar to be measured using a standard orifice.

Lehmannn and Zahn measured the dewar temperature and pressure and tracked the He inventory using the mass flow rate measured at the exit. They calculated the wetted wall area in the dewar from the He mass assuming stratified liquid and vapor. An energy balance was used to calculate the heat input into the dewar, and the wall heat flux was calculated based on the heat input and dewar wetted area. The maximum reported wall heat flux during the loss of insulation event was 3.8 watt per square centimeter $(W/cm)^2$.

Cavallari et al. [ref. 2] performed loss of vacuum tests on a vented 180-liter dewar with no superinsulation. They used a fast-opening, 80-mm inner diameter valve to create the sudden loss of vacuum. In their test, half of the He charge was vented within 1.2 seconds. They calculated the dewar heat load from a simple well-mixed thermodynamic model of the He and the measured dewar temperature and pressure. They reported a maximum heat flux of ≈4 W/cm^2. The peak heat flux occurred within the first 0.5 seconds as the measured dewar pressure increased from 120 to 500 kPa. The peak heat flux was consistent with Lehmann and Zahn's results. However, insufficient information was provided in the paper to assess their heat-flux calculation or the reported value of ≈4 W/cm^2.

Harrison [ref. 3] performed a careful, well-instrumented loss of vacuum tests on a non-superinsulated closed 12-liter superfluid He dewar in support of the space-based Alpha Magnetic Spectrometer Project. A fast-opening, 40-mm inner diameter valve was used to create the sudden loss of vacuum. After the loss of vacuum, the He passed through the lambda (λ) point (5.04 kPa) within 2 seconds and became supercritical by 3.5 seconds. At 4.5 seconds, the pressure became high enough that the dewar burst disk relieved at 1100 kPa.

The wall heat flux during the unvented portion of the test was calculated from the change in internal energy, which was based on the measured dewar temperatures and pressure. The highest calculated wall heat flux prior to the relief event was 3.1 W/cm^2, which occurred during the period where the He was supercritical.

During the time that the He was below the critical point and was two-phase, the heat flux ranged from 2.0 to 2.5 W/cm^2. This is ~60 percent of Lehmannn and Zahn's maximum. However, Harrison's dewar was unvented and boiling was inhibited. If the vessel had been open, the removal of vapor would have allowed more vigorous boiling at the walls and would likely have yielded higher heat transfer rates.

Savage et al. [ref. 4] performed loss of vacuum tests in support of the SOFIA Program on a vented, 10-liter LHe dewar with no superinsulation. The sudden loss of vacuum was provided by a 22.3-mm diameter air inlet. The dewar discharge was an open, 11.4-mm inner diameter tube and 0.36-m long. Smaller tubes of two different diameters were inserted into the discharge tube to provide a variable outlet flow restriction and a pitot to measure the total pressure near the discharge tube inlet. The static pressure near the discharge tube outlet was also measured. However, the dewar temperature was not measured. In the three tests with the pitot tube, the dewar emptied within 10 seconds. Peak pressures approaching 1000 kPa that were well above the critical pressure of 227.5 kPa were measured during the transient.

Savage et al. performed an analysis to calculate the heat flux into the dewar at the point of maximum pressure, where the time rate change of pressure was zero. The heat-flux calculation methodology was developed by Smith [ref. 5].

To calculate the mass flow rate through the discharge tube:

- The He in the dewar was assumed a homogeneous ideal gas at 6 K.
- The velocity in the discharge tube was assumed to be the acoustic velocity of He as an ideal gas at 6 K.
- A value for an intermediate pressure, p, was assumed, which was lower than the peak dewar pressure, p_0.
- The mass flow rate through the discharge tube was calculated by assuming a 0.9 tube flow coefficient and an effective density at 6 K and $\frac{p+p_\infty}{2}$, where p_∞ is the external pressure.
- The tube frictional pressure drop, $\Delta p_{friction}$, was then calculated using standard incompressible flow techniques at the calculated mass flow rate, using properties for He as an ideal gas at the same effective density and at 6 K.
- The frictional pressure drop and assumed intermediate pressure were summed and compared to the measured peak dewar pressure.
- The intermediate pressure was then adjusted until the calculated dewar pressure matched the measured peak value.

$$p_0 = p + \Delta p_{friction} \quad \text{Eq. (1)}$$

The resulting mass flow rate, $\dot{m}$, was used to calculate the wall heating, Q, from an ideal gas energy balance.

$$Q = c_p \dot{m} T \qquad \text{Eq. (2)}$$

where c_p was taken as the monatomic ideal gas specific heat and T is the assumed dewar temperature of 6 K. The ratio of the wall heating and the dewar surface area yielded the heat flux. The calculated heat fluxes at the peak dewar pressure ranged from 2.9 to 3.36 W/cm^2. These results were used as the basis of the SOFIA loss of vacuum insulation heat flux requirement of 3.7 W/cm^2 [ref. 6].

This calculation of the mass flow rate and accompanying heat flux is problematic for a number of reasons:

1. *Supercritical fluids near the critical point cannot be represented accurately as ideal gasses.* The ideal gas assumption was used to calculate the acoustic velocity, was included in the calculation of the fluid density in the vent path, and was used to determine the wall heating from the calculated mass flow rate.
2. *The assumption of 6 K He – while thought by Smith to be conservative – has no physical basis.* The temperature at the peak pressure will be set by the physical configuration of the dewar and its vent stack plus the history of the transient. The temperature at the peak pressure has a wide range of possible values (as is discussed later in this section).
3. *The calculation of the discharge tube mass flow rate is lacking in rigor*. The assumed effective density and the 0.9 flow coefficient have no identified physical basis.
4. *Calculating a frictional pressure drop using incompressible flow relations is not appropriate.* The flow in the vent tube can be compressible.
5. *Adding a frictional pressure drop to an assumed intermediate pressure has no identified physical basis.*

Because of the identified issues with the methodology used by Savage et al. to calculate wall heat flux from their experiments, their reported heat fluxes of 2.9 to 3.36 W/cm^2 must be discounted.

An attempt was made to recover useful results from Savage et al.'s tests. Savage [ref. 7] provided hard copy graphs of the pressures measured by the inserted pitot tube in each of their three experiments. A typical graph is shown in Figure 5.1-1. The graphs for all the tests are similar. They show a nearly linear increase in pressure until ~80 percent of the critical pressure is reached. The pressurization rate then increases by nearly an order of magnitude and the pressure rises into the supercritical region. The critical pressure is typically exceeded approximately 0.5 seconds after the loss of vacuum insulation.

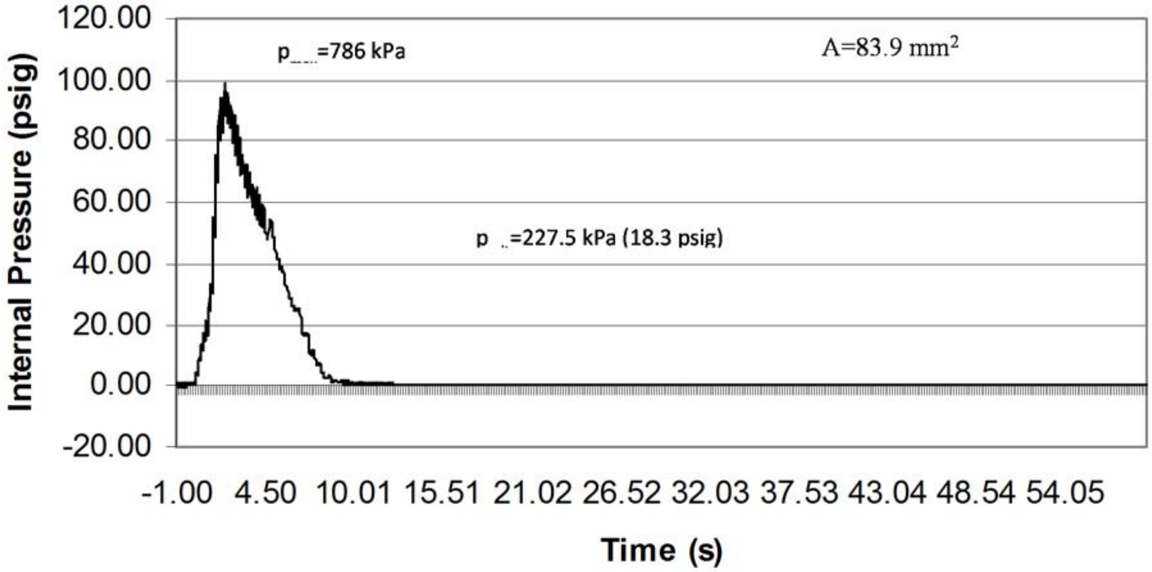

Figure 5.1-1. Pressure Trace during Loss of Insulation – from Savage [ref. 7]

During Savage et al.’s tests, the dewar He went through three distinct states: two-phase, compressed liquid, and supercritical fluid. The sequence of Savage et al.’s experiments is shown on a REFPROP[1] [ref. 8] generated pressure-internal energy diagram (Figure 5.1-2). The He started in a stratified saturated two-phase condition at 101 kPa. There was little vapor (by mass) present at the starting condition, so the dewar quality was near zero. Once the insulation vacuum was broken and heating began, the He began to boil and the pressure (and accompanying saturation temperature) in the dewar rose. Owing to the decrease in LHe density with increasing temperature, He vapor was forced out of the discharge tube. During this process, the vapor mass fraction in the dewar would have remained small, maintaining near zero dewar quality. Thus, the He state moved upwards close to the liquid side of the vapor dome (the path shown in red). At ~80 percent of the critical pressure, the slope of the pressurization increased sharply. This likely occurred after all the vapor was expelled by the liquid expansion, resulting in a liquid packed dewar. Soon, the critical pressure was exceeded and the He became a supercritical fluid. The venting continued as the He pressure increased. The range of possible peak pressure supercritical states is shown on the pressure-internal energy diagram. The leftmost bound is the liquid density at 80 percent of the critical pressure, and the lower bound is the critical pressure.

[1] National Institute of Standards and Technology thermophysical property database.

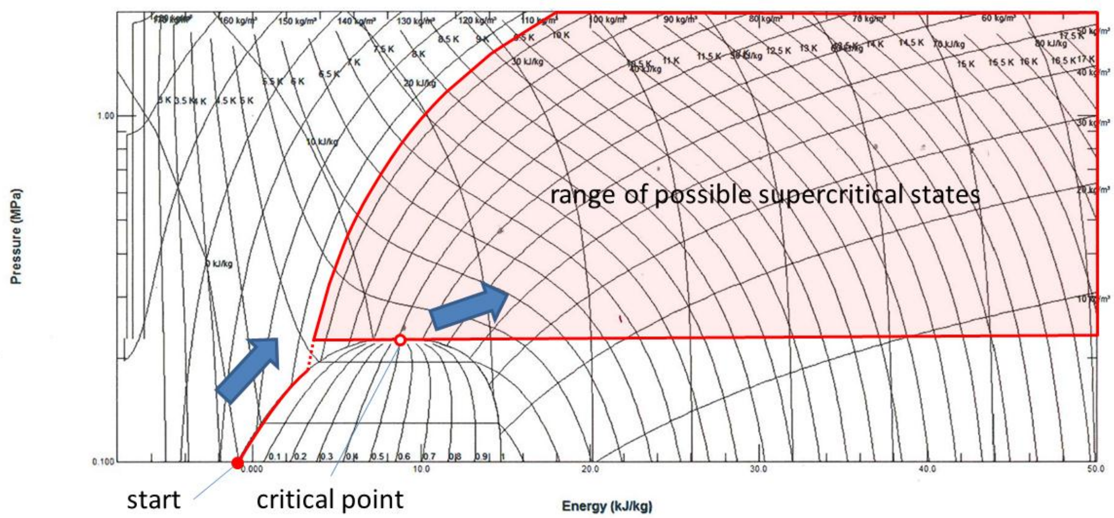

Figure 5.1-2. He Pressure-Internal Energy Diagram with Lines of Constant Temperature and Enthalpy

As Savage et al. measured only dewar pressure, the He state can be known only in the two-phase region. The He is a supercritical fluid at the peak pressure, so two parameters are required to define its state. Even though the peak dewar pressures in the tests are known, there is a wide range of possible supercritical temperatures and associated states. Thus, the heat flux at the peak pressure cannot be calculated.

However, wall-heating values can be calculated during the two-phase portion of the transient because the state is known. Key results for Savage et al.'s pitot tube tests are summarized in Table 5.1-1. The values of two-phase pressure gradients prior to the large gradient increase were measured graphically for the present work.

Table 5.1-1. Data Summary for Savage et al. Tests [ref. 4]

Vent tube flow area (mm^2)	Peak pressure (kPa)	Time for peak pressure (elapsed time in seconds)	Two-phase pressure gradient below 80 percent quality (kPa/s)
70.9	1000	1.58	184
83.9	786	1.65	183
83.9	748	2.13	176

A model was built to analyze the data from the two-phase portion of the transients. The dewar was modeled as a 10-liter volume with a surface area of 3800 cm^2 [ref. 4]. The He inside the dewar was taken to be stratified at a constant assumed quality, with each phase being homogeneous, and with the phases in thermodynamic equilibrium. The heat input was calculated from an energy balance.

In the analysis, the He was treated as a saturated mixture with a void fraction of either 0 or 10 percent to envelop the expected test conditions. A constant time rate change of pressure based on the data was applied. Using the saturated He density, specific internal energy, and specific enthalpy saturation data from REFPROP, the mass, internal energy, and enthalpy in the dewar, and the mass flow rate of the He leaving the dewar were tracked. The heat input rate was calculated over the transient from 101 kPa to 80 percent of the critical pressure. The averages over that period are listed in Table 5.1-2. The heat input rates were within ±10 percent of the average during the transient.

Table 5.1-2. Two-Phase Results for Savage et al. Tests [ref. 4]

Vent tube flow area (mm^2)	Peak pressure (kPa)	Two-phase pressure gradient (kPa/s)	Average heat flux (W/cm^2) 0 percent void fraction	Average heat flux (W/cm^2) 10 percent void fraction
70.9	1000	184	2.90	3.06
83.9	786	183	2.89	3.05
83.9	746	176	2.78	2.93

The heat input rates calculated from the early pressurization profiles for the three test points ranged from 2.8 to 3.1 W/cm^2. The assumed void fraction had only a minor effect on the calculated heat flux.

The two-phase heat input values calculated from Savage et al.'s data were higher than Harrison's measurements in the two-phase region of 2.0 to 2.5 W/cm^2 [ref. 3], and lower than Lehmann and Zahn's measurement of 3.8 W/cm^2 [ref. 1]. While venting allowed more vigorous boiling than in Harrison's unvented experiment, the high rate of pressurization (~180 kPa/s) would have hindered the boiling and reduced the heat transfer rate below that seen in Lehmann and Zahn's experiment.

Limits of Heat Transfer

After a sudden loss of vacuum insulation, there are two limits to the heat flux on a LHe dewar: the limit of energy that can be supplied by the condensation and freezing of the incoming air and the He energy uptake limit. That is, the He can absorb energy up to its physical limit, but cannot absorb more than is available from the condensing and freezing air. There are two different He heat transfer limits: a boiling limit when the dewar pressure is two-phase and a convective limit when the He is single phase – either as a compressed liquid or as a supercritical fluid.

<u>Available Energy Limit</u> - The incoming air will condense and freeze on the dewar surface, changing state from a gas at room temperature to a solid at LHe temperatures. An absolute upper limit of this heat transfer can be calculated using a technique suggested by Gambill and Lienhard [ref. 9]. The technique assumes that the air molecules travel towards the surface at mean molecular speed and are completely condensed. Using air at ambient conditions, the calculated limit is more than two orders of magnitude higher than the 2 to 4 W/cm^2 measured in the experiments described previously.

As solid air accumulates on the dewar outer surface, the heat flux into the dewar will be reduced by the thermal resistance of the solid air. Air freezes at 59.7 K[2]. Full condensation and air freezing to its triple point state provides 463 kJ/kg of energy[3]. Therefore, a constant 4 W/cm^2 of heat load results in a solid air buildup rate of 0.09 mm/s, based on the energy change and solid air density. A solid air layer of 0.2 mm, which would take 2.2 seconds to accrue, would impose a temperature drop of 50 K at 4 W/cm^2. This would result in an outer surface temperature of ~55 K, which is sufficient to condense and freeze air. Therefore, for the heat flux rates and critical times seen in the experiments discussed previously, the solid air buildup would not have limited the heat input to the He dewar.

If the dewar heat input is not limited by the energy transfer from the incoming air, then it must be limited by the He uptake. The heat uptake is limited by the boiling process when the He is two-phase. If the pressure rises above the critical point, the He is single phase and convection limits the heat transfer.

<u>Boiling Limit</u> - Although the boiling curve has been extensively studied using numerous working fluids, only limited LHe boiling experiments have been performed. The state of knowledge in 1965 was summarized in a National Bureau of Standards[4] Technical Note [ref. 10]. A key figure from the technical note is reproduced in Figure 5.1-3. This figure includes the test data and correlations available at that time for boiling heat flux as a function of wall superheat. It shows that the peak nucleate boiling heat flux, q_{max}, is ~1 W/cm^2. It also shows that film boiling in LHe is quite vigorous, yielding heat fluxes exceeding q_{max} at a relatively low wall superheat of approximately 20 K.

---

[2] This value and all air thermophysical properties were obtained from REFPROP [ref. 8].

[3] Although the dewar vacuum jacket pressure can be below the triple point during a sudden vacuum loss, this value can used as an approximation.

[4] Now National Institute of Standards and Technology (NIST).

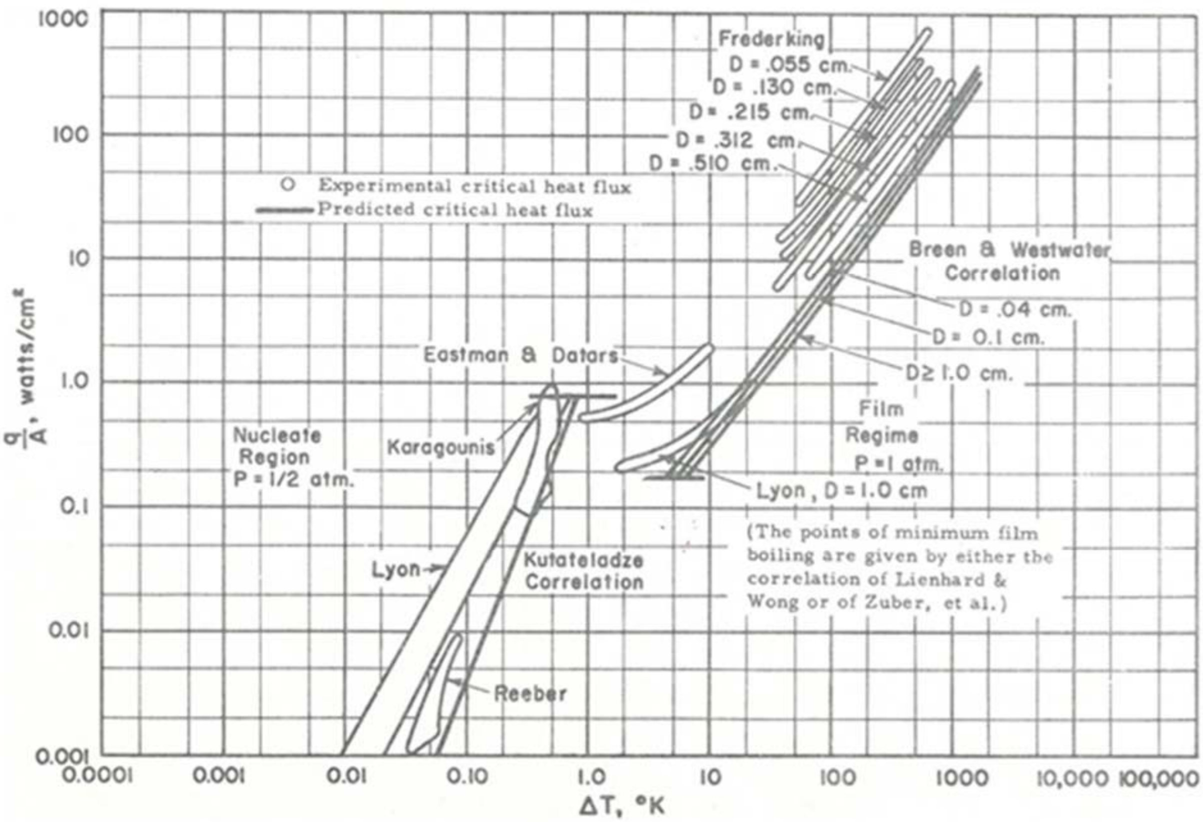

Figure 5.1-3. He Pool Boiling Curves – NIST Technical Note 317

The largest boiling heat fluxes occur at the highest wall superheat temperatures, so the dewar heat flux limit must be evaluated at the air condensation limit – the highest wall temperature where high heat fluxes are available from the air. At 101 kPa, air starts[5] to condense at 81.8 K. At higher temperatures, only sensible cooling of the air is available, so the heat transfer from the air is limited by convection. Below 81.8 K, air condensation will occur with its concomitant high heat fluxes. For LHe at 101 kPa, the saturation temperature is 4.2 K, so the maximum wall superheat with condensing air is 77.6 K, which is in the He film boiling range.

There are three studies that have measured the pool film boiling curve for LHe on horizontal large[6] electrically heated plates. Lyon [ref. 11] reported film boiling data for 101 kPa and near the critical point. Deev et al. [ref. 12] measured film boiling over a range of pressures from 101 kPa to near the critical point. Iwamoto et al. [ref. 13] obtained film boiling curves at 101 kPa.

The summary film boiling data chart from Deev et al. is reproduced in Figure 5.1-4. The original figure includes Lyon's data and Deev et al.'s data. Iwamoto et al.'s data have been added to the

[5] Because air is a multi-component mixture, it has a condensation temperature range rather than a single value.

[6] Large relative to the bubble release spacing.

chart. The data from the three experiments are consistent. The figure also shows that the film boiling curve is relatively unaffected by pressure.

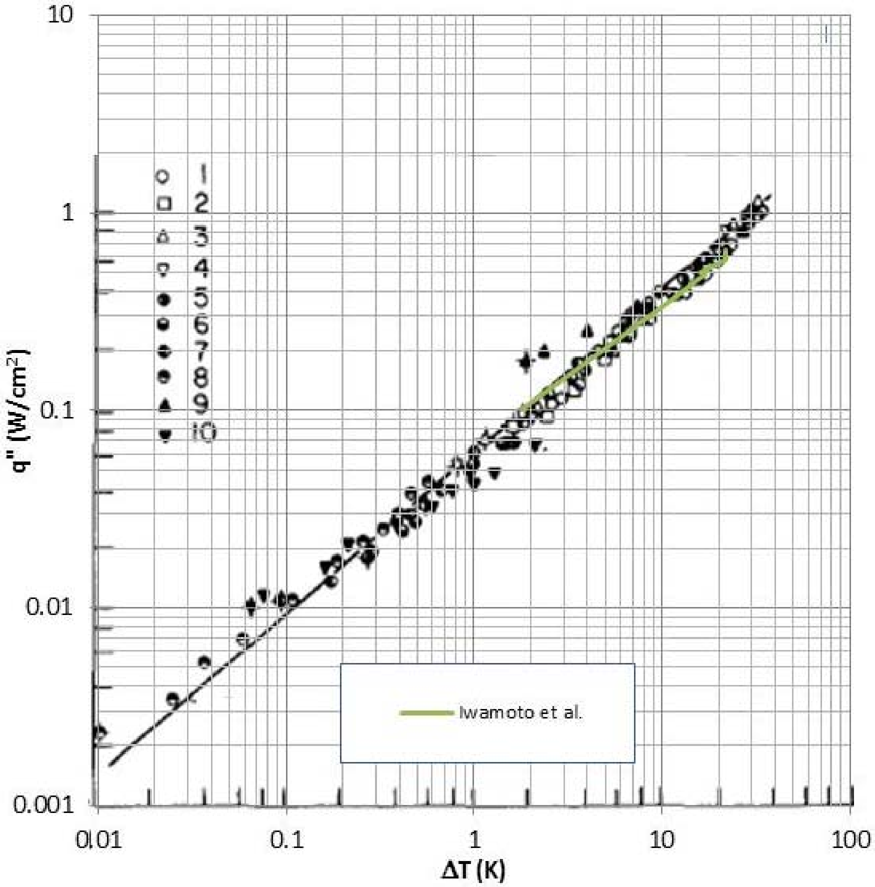

Film boiling heat transfer. Experimental data for horizontal surfaces at various pressures P, 10^5 N m^{-2}: authors data: 1 – 1.0; 2 – 1.22; 3 – 1.42; 4 – 1.62; 5 – 1.82; 6 – 2.03; 7 – 2.13; 8 – 2.23. Lyon's data:[1] 9 – 1.0; 10 – 2.15

Figure 5.1-4. Film Boiling from a Flat Plate – Various Pressures – from Deev et al. (Iwamoto's data have been added)

There is no experimental LHe film boiling data available at superheat temperatures above 35 K, so a theoretical model must be used to assess the heat flux at the 77.6 K superheat air condensation limit. Figure 5.1-5 shows the experimental data and Breen and Westwater's [ref. 14] well-accepted horizontal flat plate film boiling prediction at 101 kPa. The prediction is consistent with the data. The limiting wall superheat of 77.6 K and the 3.8 W/cm^2 maximum heat flux measured by Lehmannn and Zahn are also shown in Figure 5.1-5.

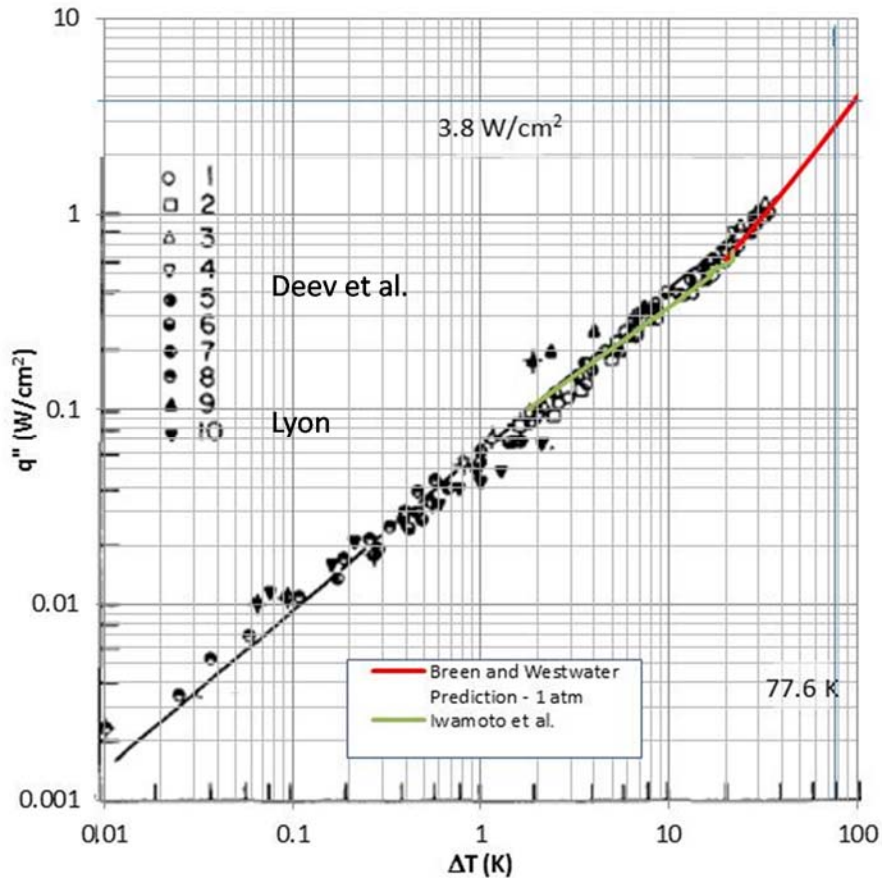

Figure 5.1-5. Film Boiling from a Flat Plate – Various Pressures

Lehmannn and Zahn's experimental result is 25 percent higher than Breen and Westwater's prediction at 77.6 K superheat. However, in a LHe dewar, only the bottom is acting as a horizontal flat plate. The dewar sides behave like vertical walls and would have a higher heat flux [ref. 13]. Thus, Lehmann and Zahn's experimental result of 3.8 W/cm^2 represents a heat flux limit that is consistent with the physical limits of film boiling heat transfer into the dewar.

<u>Supercritical Limit</u> – The heat transfer in a closed He dewar in the supercritical region was measured by Harrison [ref. 3] in his loss of vacuum tests. The experimental value of 3.1 W/cm^2 that was calculated over a pressure range from 500 to 1000 kPa is 3 to 8 times that which would be expected based on standard steady-state natural convection relations for a vertical wall and flat plate[7]. However, the characteristic conduction distance into the LHe over the timescale of Harrison's experiment is small. For the 1-second supercritical duration, the characteristic conduction distance is approximately 0.2 mm. As a result, transient effects could have played a

[7] The steady-state natural convection heat transfer was calculated using standard correlations based on Harrison's test conditions and dewar dimensions. For a 0.4-m vertical wall at 82 K in He at 6 K and 500 kPa, the steady-state natural convection heat flux would be predicted to be ~0.4 W/cm^2. For a 0.2-m horizontal heated disk at the same conditions, the steady-state heat flux would be predicted to be ~1 W/cm^2.

large role in the heat transfer. Therefore, Harrison's measured value of 3.1 W/cm^2 is an experiment-specific result that demonstrates that heat fluxes in the supercritical region can approach the film boiling limits.

Summary

A limit of 4 W/cm^2 should be used in loss of insulation calculations in the He two-phase region. This value envelopes the experimentally measured heat flux limits and is consistent with the physical limits of heat transfer in the dewar. Using 4 W/cm^2 provides a 5 percent margin on Lehmann and Zahn's experimentally determined value of 3.8 W/cm^2, which was obtained in a well-designed, well-instrumented experiment.

In addition, the limit of 4 W/m^2 should be used for loss of insulation calculations in the supercritical region. This value provides a 20 percent margin over Harrison's configuration-specific measurement of 3.1 W/cm^2.

<u>The Effect of Superinsulation</u> - The 4 W/cm^2 limit is derived from experiments on LHe dewars without superinsulation. The SOFIA dewars are superinsulated with multiple layers of aluminized Mylar, which provides a resistance to airflow and heat transfer that is not included in the suggested limit. Lehmann and Zahn measured a heat flux of 0.8 W/cm^2 in their tests on dewars with 10 layers of superinsulation. This represents a 79 percent reduction from the 3.8 W/cm^2 heat flux measured on an uninsulated dewar. Harrison reported an average heat flux of 0.44 W/cm^2 after loss of vacuum when the dewar was insulated with 3 mm of Cryocoat Ultralight® insulation. This is an 86-percent reduction from the highest uninsulated supercritical heat flux of 3.1 W/cm^2. These results demonstrate the significant effect of superinsulation on heat transfer during a sudden loss of vacuum insulation. However, since the details of superinsulation configurations are dewar specific, the 79 to 86 percent reduction cannot be applied universally. It can only be taken as an order of magnitude indicator of the superinsulation effect.

5.2 Maximum Dewar Pressure Following Loss of Vacuum

The maximum pressure that would occur following a sudden loss of vacuum insulation is critical safety-related dewar design information. This information is used to design the relief vent stack and sets the maximum acceptable dewar pressure. The SOFIA Program identified Smith's method [ref. 5] to calculate the peak dewar pressure that would occur following a sudden loss of vacuum insulation. The inverse version of Smith's method used by Savage et al. was described in the beginning of Section 5.1.

Smith's methodology follows:

- The He mass flow rate, $\dot{m}$, is calculated from

$$\dot{m} = \frac{Q}{c_p T} \qquad \text{Eq. (3)}$$

where Q is the dewar heat load, c_p is the monatomic ideal gas specific heat, and T is the absolute temperature, which is assumed to be 6 K. This is a complete energy balance representation for a venting control volume containing an ideal gas.

- The velocity in the discharge tube is assumed to be the acoustic velocity of He as an ideal gas at 6 K.
- A value for an intermediate pressure, p, is assumed and the mass flow rate through the discharge tube is calculated by assuming a 0.9 tube flow coefficient and an effective density at 6 K and $\frac{p+p_\infty}{2}$ (where p_∞ is the external pressure).
- The intermediate pressure is adjusted until the calculated mass flow rate matches the value calculated from the energy balance.
- The tube frictional pressure drop, $\Delta p_{friction}$, is then calculated using standard incompressible flow techniques:
  - at the calculated mass flow rate, and
  - using properties for He as an ideal gas at the same effective density as above and at a temperature of 6 K.
- The frictional pressure drop and assumed intermediate pressure are summed and taken as the peak dewar pressure, p_0:

$$p_0 = p + \Delta p_{friction}$$

As was previously detailed, Smith's methodology has numerous physical issues and cannot be expected to yield reliable predictions of the peak dewar pressure. A physically-based methodology was therefore developed.

Pseudo-Latent Heat

All SOFIA LHe dewars contain a pressure-relief device. Their normal operating pressures range from below the λ point (5.04 kPa) to approximately 101 kPa. These pressures are well below the critical pressure of 227.5 kPa, so the He is two-phase. In the event of a sudden vacuum loss, the wall heat flux will increase the dewar pressure until the relief system actuates. Since the relief pressure is above ambient (and is well above the λ pressure), the He will not be superfluid at this point. It will be either a two-phase mixture or a supercritical fluid, depending on the relief pressure.

Using an energy balance on a venting control volume, the venting mass flow rate, $\dot{m}$, can be expressed as:

$$\dot{m} = \frac{Q}{h_{fg}^*} \qquad \text{Eq. (4)}$$

where h_{fg}^* is a pseudo-latent heat that includes the effect of the internal energy change in the dewar. By defining h_{fg}^* appropriately, Eq. 4 can be used for both the two-phase and the supercritical cases. Of course, there is no vaporization in the supercritical case. The supercritical pseudo-latent heat is simply a convenient method of calculating the discharge mass flow rate.

At the peak pressure during the transient, the time rate change of pressure is zero $\left(\frac{dp}{dt} = 0\right)$, so the pseudo-latent heat is derived for this condition. Homogeneous conditions for all phases and thermodynamic equilibrium in the dewar are assumed in the derivation. The derivations of the two-phase and supercritical pseudo-heats of vaporization are provided in Appendix A.

For the two-phase case, assuming that only vapor exits the control volume, the pseudo-latent heat is:

$$h_{fg}^{*} = \frac{h_{fg}}{\left(1 - \frac{\rho_g}{\rho_f}\right)} \qquad \text{Eq. (5)}$$

where h_{fg} is the heat of vaporization, and ρ_f and ρ_g are the saturated liquid and vapor densities, respectively.

For the supercritical case, the pseudo-latent heat is:

$$h_{fg}^{*} = v \left.\frac{dh}{dv}\right|_{p} \qquad \text{Eq. (6)}$$

where v is the specific volume of the fluid and h is its enthalpy. As stated previously, both these results are for thermodynamic equilibrium with homogeneous conditions in each phase at the peak pressure where $\frac{dp}{dt} = 0$.

Peak Pressure Calculation

Given the wall heat flux plus the dewar and vent-stack design, the peak pressure that results from a sudden loss of vacuum insulation can be found through iteration. A peak pressure is first assumed.

If the assumed peak pressure is less than the critical pressure, the state of the dewar contents is known and the mass flow rate through the vent stack is calculated based on the dewar pressure, He vapor state, and the vent-stack configuration.

The wall heating required to create the calculated mass flow rate is then determined using the pseudo-latent heat at the assumed peak pressure. The ratio of the wall heating and the dewar surface area yields the wall heat flux.

The wall heat flux is compared to the specified wall heat flux of 4 W/cm^2. The assumed peak dewar pressure is then adjusted until the two heat flux values agree.

If the assumed dewar pressure is supercritical, the wall heat flux required to yield the assumed dewar pressure must be assessed over a range of possible dewar temperatures. The minimum of these heat fluxes is then compared to the specified wall heat flux of 4 W/cm^2. The minimum is chosen because it is conservative, it is the lowest wall heat flux that can result in the assumed pressure. The assumed supercritical dewar pressure is then adjusted until the calculated minimum equals 4 W/cm^2.

SOFIA Dewar Calculations

Because SOFIA dewars have already been accepted, the specific problem addressed in this assessment was to calculate the maximum allowable heat flux into the dewars under two conditions: at the relief pressure and at the tested proof pressure. Normally, only the first case is considered, but because the dewars have already been accepted based on the SOFIA methodology (i.e., Smith's), the tested proof pressure case was also assessed.

The analysis strategy was simpler than the iterative peak pressure procedure described previously. Analyses were performed only at the pressures of interest. The wall heat fluxes that could result in the analyzed pressures were then compared to the 4 W/cm^2 value.

The first two dewar analyses performed are described in detail to demonstrate the methodology and outline typical results. Since the other SOFIA dewars and vent stacks are physically similar, they were analyzed in a similar fashion.

The field-imaging far-infrared line spectrometer (FIFI-LS) contains two dewars: one with LHe at near-ambient pressure and one with superfluid He. Both dewars have relief stacks that terminate in burst disks. The burst disks vent to the pressurized aircraft cabin.

Key dimensions and design parameters of the FIFI-LS dewars are listed in Table 5.2-1.

Table 5.2-1. FIFI-LS Dewar Parameters

	FIFI-LS LHe	**FIFI-LS LHe II**
Normal condition	LHe at 101 kPa	superfluid He at 5 kPa
Dewar surface area (cm^2)	9208	1369
Relief pressure (kPa gage)	103	103
Equivalent relief flow diameter (mm)	26.6	26.6
Relief stack entrance	re-entrant	re-entrant
Relief stack diameter (mm)	24	11.8
Relief stack length[8] (mm)	438	442
Test proof pressure (kPa gage)	427.5	370

To calculate the mass flow rate from the vent stack at the assumed dewar conditions, a FLUINT[9] model was developed using Thermal Desktop®. The model is shown in Figure 5.2-1. It consists of two plena and an adiabatic connecting tube. The tube is divided into 11 segments. The segments closest to the plena are each 1 percent of the total length with the remainder each 10.9 percent of the total length[10]. The re-entrant inlet head-loss of 0.78 [ref. 15] is included in

[8] The stack length includes 25-mm to account for late hardware changes made to accommodate the pressure relief burst disk.

[9] SINDA/FLUINT General Purpose Thermal/Fluid Network Analyzer, Version 5.6, C&R Technologies, Littleton, Colorado, May 2013.

[10] The model nodalization was developed in consultation with the developers of the FLUINT code to maximize the accuracy and stability of the model.

the first segment. The first segment also includes a vena contracta specified as 75 percent of the tube area, which allows for choking in the vena[11].

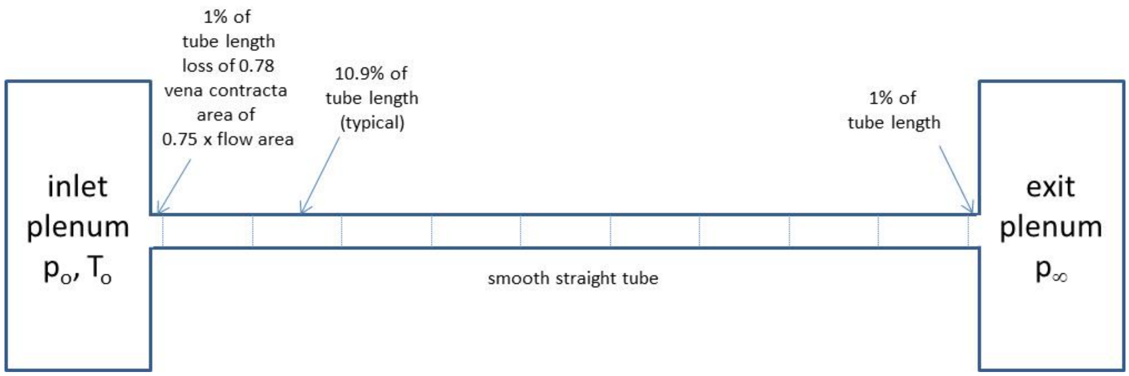

Figure 5.2-1. Thermal Desktop® Model

The conditions in the upstream plenum were based on the chosen analysis conditions. The downstream plenum was held at a specified pressure of 101 kPa for the ground condition and 75 kPa for the flight condition. He thermophysical properties were calculated within FLUINT using a real fluid (with compressible liquid) property description with heritage to REFPROP [ref. 8]. The upstream plenum contained He at one of two conditions. For a two-phase dewar, the condition was slightly superheated vapor at the specified pressure[12]; for the supercritical case, the pressure and temperature conditions were specified.

The model was exercised at the relief pressure and at the proof test pressure to calculate the venting mass flow rate over a range of conditions. The values for pseudo-latent heat at the analysis conditions were then used to calculate the wall heat flux that would result in that condition.

Cases were run for the conditions recorded in Table 5.2-2.

Table 5.2-2. FIFI-LS Case Matrix

Case	External pressure (kPa)	Internal pressure (kPa)	Dewar He state
Flight Relief Pressure	75	178	two-phase
Flight Proof Pressure	75	502.5 (FIFI-LS LHe) 445 (FIFI-LS LHe II)	supercritical
Ground Relief Pressure	101	204	two-phase
Ground Proof Pressure	101	529 (FIFI-LS LHe) 471 (FIFI-LS LHe II)	supercritical

[11] This is the incompressible flow vena contracta area for a re-entrant inlet with a 0.78 loss coefficient. Although the flow at the dewar stack entrance is compressible, the incompressible flow value was used.

[12] This avoids the numerical instability that might result from a saturated vapor boundary condition without introducing significant error.

For the two-phase cases, a single analysis was run to calculate the venting mass flow rate at the chosen pressure. The pseudo-latent heat at the dewar conditions was then used to calculate the wall heating. The ratio of the wall heating and the dewar surface area yielded the wall heat flux that would result in the chosen dewar pressure.

When the peak pressure is supercritical, the dewar temperature is a function of the heating and venting history up to that point. Because this is typically either unknown or is problematic to evaluate, the venting mass flux, pseudo-latent heat, and required wall heat flux must be evaluated over the range of possible temperatures to calculate the venting limit. The highest temperature analyzed in each configuration was at least 10 K. The lowest temperature was set by the FLUINT code limits.

For the supercritical dewar cases, the model became unstable when significant amounts of liquid were present at the vent-stack exit. As the flow entered from the supercritical plenum and passed through the vent stack, the pressure and temperature decreased. At lower supercritical plenum temperatures, the stack exit flow became two-phase. The FLUINT code was able to tolerate a small amount of liquid at the stack exit (qualities as low as 97 percent), but when the exit quality was lower, the presence of liquid produced unreliable results. This was not surprising. The physics of two-phase, low-quality, near-sonic flow are not well-understood, so the code cannot be expected to capture the true physics. This result was not important since the point of minimum required heat flux was in the range of reliable results.

No FLUINT stability limit was encountered in the two-phase dewar cases. In these cases, all the flow in the vent stack was two-phase and exit qualities as low as 80 percent were calculated successfully.

One particular temperature was included in the analysis set – the temperature corresponding to minimum $\left(1/\sqrt{v}\right)\mathrm{h}_{\mathrm{fg}}^{*}$. This condition is specified by the Compressed Gas Association Standards [ref. 16] as the point to use for relief valve sizing for supercritical dewars.

The analysis results are given in Tables 5.2-3 and 5.2-4. These tables contain the selected analysis conditions and the wall heat flux that would result in those conditions. For the supercritical dewars, the heat flux of interest was the minimum value that could result in the chosen pressure (i.e., the lowest wall heat flux that could result in the analyzed pressure). These minimum values are colored in red. The cases for minimum $\left(1/\sqrt{v}\right)\mathrm{h}_{\mathrm{fg}}^{*}$ are highlighted in yellow. The data show that the minimum required heat flux is close to that calculated at the minimum $\left(1/\sqrt{v}\right)\mathrm{h}_{\mathrm{fg}}^{*}$. In fact, evaluating the minimum heat flux solely at $\left(1/\sqrt{v}\right)\mathrm{h}_{\mathrm{fg}}^{*}$ would have resulted in a difference of only 1 percent. However, the four analysis cases discussed here are not sufficient to state whether only a single analysis case at minimum $\left(1/\sqrt{v}\right)\mathrm{h}_{\mathrm{fg}}^{*}$ is sufficient to assess the dewar pressure after a sudden loss of insulation vacuum. More analysis cases for different stack designs over a wide range of dewar pressures would be required to suggest a single temperature for future analyses.

Table 5.2-3. FIFI-LS LHe Wall Heat Flux

p_o (kpa)	T_o (K)	p_∞ (kPa)	mass flow rate (kg/s)	condition	h_{fg}* (kJ/kg)	Q (W)	q (W/cm^2)
178	4.90	75	0.53	x > 0.80 - choke at inlet	21.00	11129.9	1.21
502.5	7.00	75	1.471	no liquid - choke at inlet and exit	24.34	35809.1	3.89
502.5	7.08	75	1.427	no liquid - choke at inlet and exit	24.82	35418.1	3.85
502.5	7.50	75	1.282	no liquid - choke at inlet and exit	27.31	35011.4	**3.80**
502.5	8.00	75	1.168	no liquid - choke at inlet and exit	30.73	35892.3	3.90
502.5	9.00	75	1.055	no liquid - choke at inlet and exit	37.59	39661.9	4.31
502.5	10.00	75	0.935	no liquid - choke at inlet and exit	44.21	41338.9	4.49
204	5.10	100	0.6126	x > 0.82 - choke at inlet	19.00	11639.1	1.26
529	7.00	101	1.6	97% exit quality - choke at inlet and exi	24.62	39392.0	4.28
529	7.10	101	1.529	no liquid - choke at inlet and exit	24.95	38144.0	4.14
529	7.22	101	1.489	no liquid - choke at inlet and exit	25.66	38207.7	4.15
529	7.50	101	1.383	no liquid - choke at inlet and exit	27.38	37866.5	**4.11**
529	8.00	101	1.251	no liquid - choke at inlet and exit	30.55	38217.3	4.15
529	9.00	101	1.087	no liquid - choke at inlet and exit	37.33	40582.0	4.41
529	10.00	101	0.9894	no liquid - choke at inlet and exit	44.03	43564.9	4.73

Table 5.2-4. FIFI-LS LHe II Wall Heat Flux

p_o (kpa)	T_o (K)	p_∞ (kPa)	mass flow rate (kg/s)	condition	h_{fg}* (kJ/kg)	Q (W)	q (W/cm^2)
178	4.90	75	0.1244	x > 0.82 - choke at inlet	21.00	2612.4	1.91
445	6.83	75	0.3026	x > 0.997 - choke at exit	23.16	7008.5	5.12
445	6.90	75	0.2976	all vapor - choke at exit	23.57	7012.9	5.12
445	7.00	75	0.2892	all vapor - choke at exit	24.50	7085.5	5.18
445	7.50	75	0.2574	all vapor - choke at exit	27.66	7120.7	5.20
445	8.00	75	0.2382	all vapor - choke at exit	31.54	7511.8	5.49
445	9.00	75	0.213	all vapor - choke at inlet and exit	38.42	8184.2	5.98
445	10.00	75	0.1957	all vapor - choke at inlet and exit	44.95	8796.5	6.43
204	5.10	101	0.1468	x > 0.80 - choke at inlet	19.00	2789.1	2.04
471	6.80	101	0.3297	x > 0.997 - choke at exit	23.12	7622.3	5.57
471	6.90	101	0.3226	x > 0.9997 - choke at exit	23.64	7625.3	5.57
471	7.00	101	0.3127	all vapor - choke at exit	24.18	7562.5	5.52
471	7.01	101	0.3116	all vapor - choke at exit	24.31	7576.3	5.53
471	7.50	101	0.2775	all vapor - choke at exit	27.54	7643.4	5.58
471	8.00	101	0.2554	all vapor - choke at exit	31.04	7927.5	5.79
471	9.00	101	0.2275	no liquid - choke at inlet and exit	37.92	8626.9	6.30
471	10.00	101	0.2084	no liquid - choke at inlet and exit	44.56	9287.1	6.78

These tables show that the dewars cannot accommodate the 4 W/cm^2 limit at the relief pressure – the wall heat fluxes at the relief pressure range from 1.21 to 2.04 W/cm^2. At the tested proof pressure, the 4 W/cm^2 limit is accommodated by the FIFI-LS LHe II dewar and is accommodated by the FIFI-LS LHe dewar for the ground case. The FIFI-LS LHe dewar flight case can accommodate only 3.8 W/ cm^2.

The FLUINT models built within Thermal Desktop® provided results that were thermodynamically-consistent (i.e., energy balances were satisfied, entropy increased, and expected trends in temperature and pressure were followed) over the range of conditions that were required to calculate the minimum wall heat flux at each dewar pressure.

A similar analysis was run to assess Savage et al.'s loss of vacuum tests. Models were built of the two test configurations where dewar pressure was measured. The required wall heat flux was calculated for a range of dewar temperatures at the measured peak pressure. The calculated minimum heat fluxes at the measured peak supercritical pressures ranged from 2.83 to 3.45 W/cm^2. That is, at the measured peak supercritical pressure, the dewar heat load was *at least* 2.83 to 3.45 W/cm^2. These results were consistent with the identified heat flux limit of 4 W/cm^2. Details of the analyses are provided in Appendix B.

Summary

A physically complete numerical model should be used to calculate the allowable wall heat flux at the selected dewar maximum pressure. Different venting boundary conditions should be used depending on the dewar fluid state.

1. For a two-phase peak-pressure state in the dewar, a single dewar condition of saturated homogeneous stratified liquid and vapor in thermodynamic equilibrium should be analyzed. Saturated vapor is assumed to be present at the vent-stack inlet.
2. For a supercritical peak pressure state in the dewar, the model must be exercised over the range of possible dewar temperatures to allow calculation of the minimum wall heat flux required to obtain the peak pressure.

The numerical model is used to calculate the venting mass flux. The pseudo-latent heat, h^*_{fg}, at the dewar condition is then used to calculate the dewar heating. The dewar surface area is used to calculate the wall heat flux.

For the two-phase case, the calculated dewar heat flux should be compared to the 4 W/cm^2 sudden loss of vacuum insulation limit to assess the acceptability of the vent-stack design. For the supercritical case, the minimum calculated dewar heat flux should be compared to the same limit to assess the vent-stack design acceptability.

6.0 Findings, Observations, and NESC Recommendations

6.1 Findings

The following findings were identified:

F-1. A heat flux limit of 4 W/cm^2 is appropriate for use in sudden loss of vacuum insulation calculations where the condition at the peak pressure is two-phase.

- This value envelopes the experimentally measured heat flux limits and is consistent with the physical limits on heat transfer in the dewar.

F-2. A heat flux limit of 4 W/cm^2 is appropriate for loss of vacuum insulation calculations where the dewar contents are supercritical at the peak pressure.

- This value provides a reasonable margin over the sole experimentally measured heat flux limit in the literature.

F-3. A universal superinsulation knockdown factor is not practical due to the wide variation in insulation configurations.

- Although the presence of superinsulation will restrict the airflow into the vacuum jacket and reduce the wall heat flux below the uninsulated case, the wide variation in insulation configurations rules out the recommendation of a universal knockdown factor.

F-4. A physically complete numerical model can be used to calculate the maximum dewar pressure at an applied heat flux.

- The model must include the losses in the vent stack and real compressible fluid behavior. An iterative modeling approach will yield a single peak pressure in the two-phase case and a range of peak pressures (over a range of temperatures) in the supercritical case. The maximum value is the pressure limit for the supercritical case.

F-5. If the maximum dewar pressure is known, a physically complete numerical model including all the losses in the vent stack and real compressible fluid behavior can be used to calculate the wall heat flux that will create that condition.

- For the two-phase case, a single heat flux will be found and compared to the sudden loss of vacuum insulation limit. For the supercritical case, a range of heat fluxes (over a range of dewar temperatures) will be found. The minimum value will be compared to the sudden loss of vacuum insulation limit.

F-6. The FIFI-LS LHe dewar can accommodate 1.21 W/cm^2 (in flight) and 1.26 W/cm^2 (on the ground) at its relief pressure. It can accommodate 3.80 W/cm^2 (in flight) and 4.11 W/cm^2 (on the ground) at its tested proof pressure. The FIFI-LS LHe II dewar can accommodate 1.91 W/cm^2 (in flight) and 2.04 W/cm^2 (on the ground) at its relief pressure. It can accommodate 5.12 W/cm^2 (in flight) and 5.52 W/cm^2 (on the ground) at its tested proof pressure.

6.2 Observations

The following observations were made:

O-1. When performing cryogenic fluid dewar loss of vacuum insulation experiments, sufficient instrumentation must be included so that the He state can be discerned.

O-2. A complete dewar energy balance, including real fluid behavior, is required when analyzing data from cryogenic fluid dewar sudden loss of vacuum insulation experiments.

O-3. Real fluid behavior and compressibility must be considered in stack flow analyses.

6.3 NESC Recommendations

The following NESC recommendations are directed towards the SOFIA Program:

R-1. Use a heat flux limit of 4 W/cm^2 in all sudden loss of vacuum insulation calculations. This includes the case where condition at the peak pressure is two-phase and the condition where it is supercritical. ***(F-1, F-2)***

R-2. Use a heat flux limit of 4 W/cm^2 for dewars with and without superinsulation. ***(F-3)***

R-3. Use a physically complete numerical model of the dewar and vent stack, including real fluid behavior and compressibility effects, to assess the effect of a sudden loss of vacuum. ***(F-4, F-5, and O-2)***

7.0 Lessons Learned

No applicable lessons learned were identified for entry into the NASA Lessons Learned Information System (LLIS) as a result of this assessment.

8.0 Recommendations for NASA Standards and Specifications

No recommendations for NASA standards and specifications were identified as a result of this assessment.

9.0 Definition of Terms

Corrective Actions	Changes to design processes, work instructions, workmanship practices, training, inspections, tests, procedures, specifications, drawings, tools, equipment, facilities, resources, or material that result in preventing, minimizing, or limiting the potential for recurrence of a problem.
Finding	A relevant factual conclusion and/or issue that is within the assessment scope and that the team has rigorously based on data from their independent analyses, tests, inspections, and/or reviews of technical documentation.
Lessons Learned	Knowledge, understanding, or conclusive insight gained by experience that may benefit other current or future NASA programs and projects. The experience may be positive, as in a successful test or mission, or negative, as in a mishap or failure.
Observation	A noteworthy fact, issue, and/or risk, which may not be directly within the assessment scope, but could generate a separate issue or concern if not addressed. Alternatively, an observation can be a positive acknowledgement of a Center/Program/Project/Organization's operational structure, tools, and/or support provided.
Problem	The subject of the independent technical assessment.
Proximate Cause	The event(s) that occurred, including any condition(s) that existed immediately before the undesired outcome, directly resulted in its occurrence and, if eliminated or modified, would have prevented the undesired outcome.
Recommendation	A proposed measurable stakeholder action directly supported by specific Finding(s) and/or Observation(s) that will correct or mitigate an identified issue or risk.
Root Cause	One of multiple factors (events, conditions, or organizational factors) that contributed to or created the proximate cause and subsequent undesired outcome and, if eliminated or modified, would have prevented the

	undesired outcome. Typically, multiple root causes contribute to an undesired outcome.
Supporting Narrative	A paragraph, or section, in an NESC final report that provides the detailed explanation of a succinctly worded finding or observation. For example, the logical deduction that led to a finding or observation; descriptions of assumptions, exceptions, clarifications, and boundary conditions. Avoid squeezing all of this information into a finding or observation

10.0 Acronyms List

λ	Lambda
CERN	The European Organization for Nuclear Research
CGA	Compressed Gas Association
cm	Centimeter
FIFI-LS	Field-Imaging Far-Infrared Line Spectrometer
He	Helium
JSC	Johnson Space Center
K	kilo
kPa	Peak Pressure
LaRC	Langley Research Center
LHe	Liquid Helium
mm	Millimeter
NASA	National Aerospace and Space Administration
NESC	NASA Engineering and Safety Center
NIST	National Institute of Standards and Technology
SOFIA	Stratospheric Observatory for Infrared Astronomy
W/cm	Watt Per Square Centimeter

11.0 References

1. Lehmannn, W.; and G. Zahn: "Safety Aspects for LHe Cryostats and LHe Transport Containers." *7th Int'l Cryogenic Enrg. Conf.*, London, July 4-7, 1978, pp. 569-579.

2. Cavallari, G.; Gorine, I.; Gusewell, D.; and Stierlin, R.: "Pressure Protection Against Vacuum Failures on the Cryostats for LEP SC Cavities." *Proc. 4th Workshop on RF Superconductivity, KEK*, Tsubaka, Japan, August 1989, pp. 781-803.

3. Harrison, S.: "Loss of Vacuum Experiments on a Superfluid He Vessel." *Scientific Magnetics*, September 24, 2001.

4. Savage, M. L.; Limmongkol, S.; Bacher, R. E.; Brown, T. M.; Koerber, C. T.; Smith, E.; and Waddell, P.: "He Cryostat Vent Sizing for SOFIA Science Instruments." *Ground Based Instrumentation for Astronomy, Proc. of the SPIE*, Vol. 5492, 2004, pp. 1689-1698.

5. Smith, E.: *Design of Dewar Neck for Safe Depressurization, Under Catastrophic Vacuum Failure in Jacket*. October 11, 2001, revision, provided by M. L. Savage, March 2014.
6. PRG-CCR-073A, Qualification Pressure Factor for Science Instrument Cryostat Cryogen Reservoirs and PVS From:/To: changes relative to SE01-2028 Rev., 18 April 2011.
7. Savage, M. L.: Private Communication, September 2013.
8. Lemmon, E. W.; Huber, M. L.; and McLinden, M. O.: *NIST Standard Reference Database 23: Reference Fluid Thermodynamic and Transport Properties-REFPROP*. Version 9.1, NIST, Standard Reference Data Program, Gaithersburg, 2013.
9. Gambill, W. P.; and Lienhard, J. H.: "An Upper Limit for the Critical Boiling Heat Flux." *ASME Journal of Heat Transfer*, Vol. 111, 1989, pp. 815-818.
10. Brentari, E. G.; Giarratano, P. J.; and Smith, R. V.: *Boiling Heat Transfer for Oxygen, Nitrogen, Hydrogen, and He*. National Bureau of Standards Technical Note 317, 1965.
11. Lyon, D. N.: "Boiling Heat Transfer and Peak Nucleate Boiling Heat Fluxes in Saturated Liquid He Between the λ and Critical Temperatures." *International Advances in Cryogenic Engineering*, Vol. 10, 1965, pp. 371-379.
12. Deev, V.; Keillin, K; Kondratenko, A.; and Petrovichev, V.: Nucleate and Film Pool Boiling Heat Transfer to Saturated Liquid He. *Cryogenics*, October 1977, pp. 557-562.
13. Iwamoto, A.; Mito, T.; Takahata, K.; Yagani, N.; and Yamamoto, J.: "Heat Transfer of a Large Copper Plate to Liquid He Applicable to Large Scale Superconductors." *Cryogenics*, Vol. 34, ICEC Supplement, 1994, pp. 321-324.
14. B. P. Breen and J. W. Westwater, "Effect of Diameter of Horizontal Tubes on Film Boiling Heat Transfer," Chem. Eng. Prog., Vol. 58, No. 7, July 1962, pp. 67-72.
15. Sabersky, R. H., Acosta, A. J., and Hauptman, E. G., Fluid Flow, A First Course in Fluid Mechanics, Second Edition, Macmillan, New York, 1971.
16. Compressed Gas Association, CGA S-1.3-2008, Pressure Relief Device Standards – Part 3 – Stationary Storage Containers for Compressed Gases.

12.0 Appendices

Appendix A. Derivation of Pseudo-Latent Heats

Two-Phase Venting Tank with $\frac{dp}{dt} = 0$

Consider the venting tank shown in Figure A-1. The tank contains a two-phase stratified mixture at pressure, p, in thermodynamic equilibrium. Each phase is homogeneous. The tank vents vapor through a relief stack. The properties of the fluid in the tank are represented by h as enthalpy, m as mass, and ρ as density. The subscripts f and g represent the liquid and vapor phases, respectively.

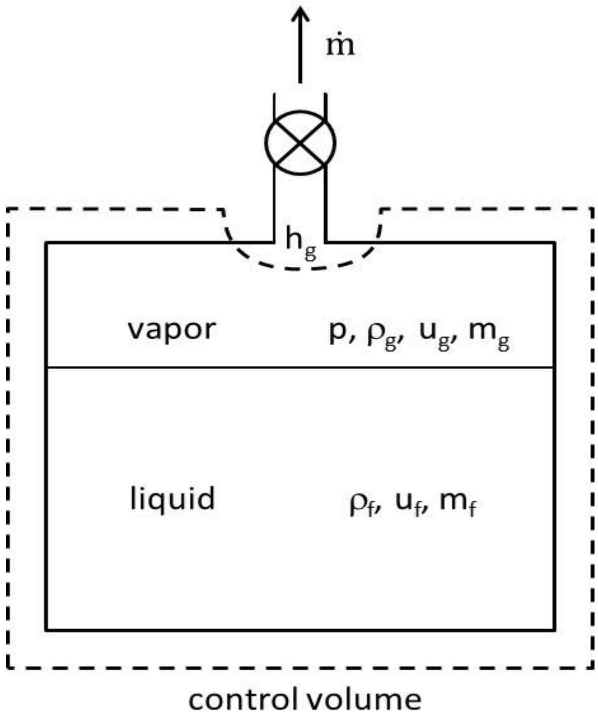

Figure A-1. Control Volume for Two-Phase Venting Tank

The control volume for the system is shown in the diagram. Taking part of the control volume border inside the tank creates a negligible error in the representation of the fluid mass, but simplifies the energy equation by minimizing the fluid kinetic energy term and allowing it to be neglected.

<u>Mass Balance</u> - The mass balance on the control volume is based on the change of liquid volume, ΔV_f, in the tank. The change in liquid volume is mirrored by the change in vapor volume, ΔV_g,:

$$\Delta V_f = -\Delta V_g,$$

which can be expressed as changes in the masses of liquid and vapor:

$$\frac{\Delta m_f}{\rho_f} = -\frac{\Delta m_g}{\rho_g}.$$

Since $\frac{dp}{dt} = 0$, the derivatives of ρ_f and ρ_f with respect to time are zero. The relative time (t) rates of change of the masses of each phase are:

$$\frac{1}{\rho_f}\frac{dm_f}{dt} = -\frac{1}{\rho_g}\frac{dm_g}{dt},$$

so

$$\frac{dm_f}{dt} = -\frac{\rho_f}{\rho_g}\frac{dm_g}{dt},$$

and

$$\frac{dm_g}{dt} = -\frac{\rho_g}{\rho_f}\frac{dm_f}{dt}.$$

The net mass flow rate out of the tank, $\dot{m}$, is:

$$\dot{m} = -\frac{dm}{dt} = -\frac{d}{dt}\left(m_f + m_g\right),$$

$$\dot{m} = -\frac{dm_f}{dt} - \frac{dm_g}{dt},$$

$$\frac{dm_f}{dt} < 0 \;\; and \;\; \frac{dm_g}{dt} > 0.$$

$\dot{m}$ can be expressed in terms of the change of vapor mass in the tank:

$$\dot{m} = \frac{\rho_f}{\rho_g}\frac{dm_g}{dt} - \frac{dm_g}{dt},$$

so

$$\dot{m} = \frac{dm_g}{dt}\left(\frac{\rho_f}{\rho_g} - 1\right),$$

and

$$\frac{dm_g}{dt} = \frac{\dot{m}}{\frac{\rho_f}{\rho_g} - 1}.$$

Alternately, $\dot{m}$ can be expressed in terms of the change of liquid mass in the tank:

$$\dot{m} = -\frac{dm_f}{dt} + \frac{\rho_g}{\rho_f}\frac{dm_f}{dt}$$

$$\dot{m} = -\frac{dm_f}{dt}\left(1 - \frac{\rho_g}{\rho_f}\right)$$

$$\frac{dm_f}{dt} = \frac{\dot{m}}{1 - \frac{\rho_g}{\rho_f}}.$$

Energy Balance - An energy balance can be performed on the tank where Q is the heat input, U is the fluid internal energy, h is the fluid specific enthalpy, and v is the fluid specific volume. Because of the way that the control volume is drawn in Figure A-1, the kinetic energy of the exiting flow is small and can be neglected and:

$$Q = \frac{dU}{dt} + \dot{m}h.$$

The internal energy of the tank contents is:

$$U = m_f u_f + m_g u_g.$$

Since $\frac{dp}{dt} = 0$, the derivatives of u_f and u_g with respect to time are zero and

$$\frac{dU}{dt} = \frac{dm_f}{dt}u_f + \frac{dm_g}{dt}u_g.$$

The rate of enthalpy leaving the tank is

$$\dot{m}h = \left(-\frac{dm_f}{dt} - \frac{dm_g}{dt}\right)h_g$$

where

$$h_g = u_g + pv_g$$

so

$$Q = \frac{dm_f}{dt}u_f + \frac{dm_g}{dt}u_g + \dot{m}h_g$$

For convenience, define:

$$r = \frac{\rho_f}{\rho_g}$$

$$Q = -\frac{\dot{m}}{1 - \frac{1}{r}}u_f + \frac{\dot{m}}{r - 1}u_g + h_g.$$

Define a pseudo-latent heat, h_{fg}^{*}, as:

$$h_{fg}^{*} = \frac{Q}{\dot{m}}.$$

So

$$h_{fg}^{*} = -\frac{u_f}{1-\frac{1}{r}} + \frac{u_g}{r-1} + h_g$$

since

$$r - 1 = r\left(1 - \frac{1}{r}\right)$$

$$h_{fg}^{*} = -\frac{u_f}{1-\frac{1}{r}} + \frac{u_g}{r\left(1-\frac{1}{r}\right)} + \frac{h_g\left(1-\frac{1}{r}\right)}{1-\frac{1}{r}}$$

$$h_{fg}^{*}\left(1-\frac{1}{r}\right) = -u_f + \frac{u_g}{r} + h_g - \frac{h_g}{r}$$

$$h_{fg}^{*}\left(1-\frac{1}{r}\right) = h_g - u_f - \frac{1}{r}\left(h_g - u_g\right).$$

By definition

$$h_g - u_g = pv_g$$

and

$$\frac{1}{r} = \frac{\rho_f}{\rho_g} = \frac{v_f}{v_g},$$

so

$$h_{fg}^{*}\left(1-\frac{1}{r}\right) = h_g - u_f - \frac{1}{r}pv_g$$

$$h_{fg}^{*}\left(1-\frac{1}{r}\right) = h_g - u_f - \frac{v_f}{v_g}pv_g$$

$$h_{fg}^{*}\left(1-\frac{1}{r}\right) = h_g - u_f - pv_f$$

since

$$u_f + pv_f = h_f$$

$$h_{fg}^{*}\left(1-\frac{1}{r}\right) = h_g - h_f = h_{fg}.$$

The pseudo-latent heat for a two-phase venting fluid is:

$$h_{fg}^* = \frac{h_{fg}}{\left(1 - \frac{1}{r}\right)}$$

or

$$\boxed{h_{fg}^* = \frac{h_{fg}}{1 - \frac{\rho_f}{\rho_g}}.}$$

Supercritical Venting Tank with $\frac{dp}{dt} = 0$

Consider the venting tank shown in Figure A-2. The tank contains a homogeneous supercritical fluid at pressure, p. The tank vents through a relief stack. The mass of the fluid in the tank is m, its density is ρ, and its specific internal energy is u. The mass flow rate of the fluid leaving the tank is ṁ and its specific enthalpy is h.

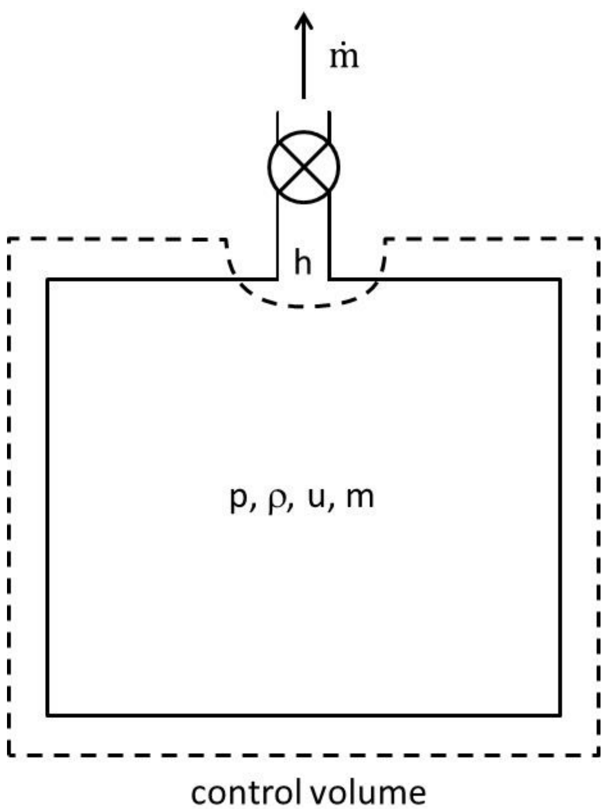

Figure A-2. Control Volume for Venting Supercritical Tank

The control volume for the system is taken as shown in the diagram. Taking part of the control volume border inside the tank creates a negligible error in the representation of the fluid mass, but minimizes the fluid kinetic energy at the exit and allows it to be neglected.

Mass Balance - The mass balance on the control volume is

$$\dot{m} = -\frac{dm}{dt}$$

where t is time.

Energy Balance – The energy balance on the control volume is:

$$Q = \frac{dU}{dt} + \dot{m}h$$

$$U = mu = m(h - p\mathit{v}).$$

The energy balance can be expressed as:

$$Q = \frac{d}{dt}[mh - mp\mathit{v}] - \frac{dm}{dt}h.$$

Expanding the energy balance

$$Q = h\frac{dm}{dt} + m\frac{dh}{dt} - mp\frac{d\mathit{v}}{dt} - m\mathit{v}\frac{dp}{dt} - p\mathit{v}\frac{dm}{dt} - h\frac{dm}{dt}.$$

Because

$$-mv\frac{dp}{dt} = 0 \text{ since } \frac{dp}{dt} = 0\,,$$

this allows the energy balance to be simplified to:

$$Q = m\frac{dh}{dt} - mp\frac{d\mathit{v}}{dt} - p\mathit{v}\frac{dm}{dt}.$$

Specific volume, v, is defined as:

$$\mathit{v} = \frac{V}{m}$$

where V is the tank volume, so

$$\frac{d\mathit{v}}{dt} = -\frac{V}{m^2}\frac{dm}{dt}$$

and

$$\frac{dv}{dt} = -\mathit{v}\frac{1}{m}\frac{dm}{dt}$$

This allows the energy balance to be recast as:

$$Q = m\frac{dh}{dt} + mpv\frac{1}{m}\frac{dm}{dt} - pv\frac{dm}{dt}$$

or

$$Q = m\frac{dh}{dt}$$

$$\frac{dh}{dt} = \frac{dh}{dv}\frac{dv}{dt} = \frac{dh}{dv}\left(-\frac{v}{m}\frac{dm}{dt}\right).$$

Recall

$$\dot{m} = -\frac{dm}{dt}$$

so

$$\frac{dh}{dt} = \frac{dh}{dv}\left(\frac{v}{m}\dot{m}\right)$$

$$Q = m\left(\frac{dh}{dv}\frac{v}{m}\dot{m}\right)$$

$$Q = \dot{m}v\frac{dh}{dv}$$

so

$$\dot{m} = \frac{Q}{v\frac{dh}{dv}}.$$

Define the pseudo-latent heat, h_{fg}^*, as:

$$h_{fg}^* = \frac{Q}{\dot{m}}$$

$$\dot{m} = \frac{Q}{h_{fg}^*}.$$

The pseudo-latent heat for a supercritical fluid is:

$$\boxed{h_{fg}^* = v\left.\frac{dh}{dv}\right|_p .}$$

Appendix B. Savage et al.'s Test Results

FLUINT models similar to the FIFI-LS dewar models were built to assess Savage et al.'s loss of vacuum tests [ref. 4]. Models were built for the two configurations where the dewar pressure was measured. The vent-stack flow area, hydraulic diameter, and stack length were incorporated in the FLUINT model. The vent tube length was 358 mm, the inner diameter was 11.4 mm, and the dewar surface area was 3800 cm^2. In the analyses, the dewar contents were assumed to be in a homogeneous condition at the peak measured pressure (p_o). The analyses were run using two entrance configurations, a re-entrant vent tube inlet and a flush tube inlet[13] to bound the physical configuration.

The model results are shown in Table B-1. In the table, the cases with minimum $\left(1/\sqrt{v}\right)h^*_{fg}$ are highlighted in yellow. The minimum wall heat flux required to obtain the measured peak pressure is red. As in the analysis for the FIFI-LS dewars, the minimum heat load is well predicted by the analysis case at the minimum $\left(1/\sqrt{v}\right)h^*_{fg}$. There is less than 6 percent difference between this value and the lowest calculated wall heat flux.

[13] The flush inlet was modeled using a loss coefficient of 0.50 [ref. 15] and a vena contracta of 82 percent of the flow area (incompressible flow result).

Table B-1. Predicted Wall Heat Flux at Peak Pressure in Savage et al.'s Experiments – at Various Temperatures

p_o (kpa)	T_o (K)	entrance	p_∞ (kPa)	mass flow rate (kg/s)	condition	h_{fg}* (kJ/kg)	Q (W)	q (W/cm^2)
998	7.00	re-entrant	101	0.474	80% quality at exit - choked	39.02	18495	4.87
998	7.50	0.78	101	0.4407	all vapor - choked at exit	37.01	16310	4.29
998	8.00	re-entrant	101	0.3998	all vapor - choked at exit	37.17	14861	3.91
998	8.05	re-entrant	101	0.3976	all vapor - choked at exit	36.07	14341	3.77
998	8.50	re-entrant	101	0.3674	all vapor - choked at exit	37.75	13869	3.65
998	9.00	re-entrant	101	0.3385	all vapor - choked at exit	39.19	13266	3.49
998	9.30	re-entrant	101	0.3246	all vapor - choked at exit	39.87	12942	3.41
998	9.50	re-entrant	101	0.3161	all vapor - choked at exit	41.69	13178	3.47
998	10.00	re-entrant	101	0.297	all vapor - choked at exit	42.12	12510	**3.29**
998	10.50	re-entrant	101	0.2833	all vapor - choked at exit	46.42	13151	3.46
998	11.00	re-entrant	101	0.271	all vapor - choked at exit	49.60	13442	3.54
998	11.50	re-entrant	101	0.2603	all vapor - choked at exit	52.81	13746	3.62
998	12.00	re-entrant	101	0.251	all vapor - choked at exit	55.30	13880	3.65
998	12.50	re-entrant	101	0.2429	all vapor - choked at exit	58.29	14159	3.73
998	13.00	re-entrant	101	0.2355	all vapor - choked at exit	61.96	14592	3.84
998	14.00	re-entrant	101	0.2231	all vapor - choked at exit	67.96	15162	3.99
998	15.00	re-entrant	101	0.2127	all vapor - choked at exit	74.45	15836	4.17
998	6.50	flush	101	0.5525	all vapor - choked at exit	41.45	22901	6.03
998	7.00	flush	101	0.5074	all vapor - choked at exit	39.02	19799	5.21
998	7.50	flush	101	0.4614	all vapor - choked at exit	37.01	17076	4.49
998	8.00	flush	101	0.4204	all vapor - choked at exit	37.17	15626	4.11
998	8.05	flush	101	0.4171	all vapor - choked at exit	36.07	15045	3.96
998	8.50	flush	101	0.3843	all vapor - choked at exit	37.75	14507	3.82
998	9.00	flush	101	0.3537	all vapor - choked at exit	39.19	13862	3.65
998	9.30	flush	101	0.3393	all vapor - choked at exit	39.87	13528	3.56
998	9.50	flush	101	0.3314	all vapor - choked at exit	41.69	13816	3.64
998	10.00	flush	101	0.3112	all vapor - choked at exit	42.12	13108	**3.45**
998	10.50	flush	101	0.2963	all vapor - choked at exit	46.42	13754	3.62
998	11.00	flush	101	0.283	all vapor - choked at exit	49.60	14037	3.69
998	11.50	flush	101	0.2706	all vapor - choked at exit	52.81	14290	3.76
998	12.00	flush	101	0.2607	all vapor - choked at exit	55.30	14417	3.79
998	12.50	flush	101	0.2522	all vapor - choked at exit	58.29	14701	3.87
998	13.00	flush	101	0.2455	all vapor - choked at exit	61.96	15211	4.00
998	14.00	flush	101	0.2314	all vapor - choked at exit	67.96	15726	4.14
998	15.00	flush	101	0.22	all vapor - choked at exit	74.45	16379	4.31
783	7.41	re-entrant	101	0.4223	all vapor - choked at exit	30.58	12914	3.40
783	7.50	re-entrant	101	0.4141	all vapor - choked at exit	30.68	12705	3.34
783	8.00	re-entrant	101	0.3691	all vapor - choked at exit	32.29	11918	3.14
783	8.17	re-entrant	101	0.3566	all vapor - choked at exit	32.39	11550	3.04
783	9.00	re-entrant	101	0.3105	all vapor - choked at exit	36.85	11442	**3.01**
783	9.30	re-entrant	101	0.2988	all vapor - choked at exit	38.46	11492	3.02
783	9.50	re-entrant	101	0.2917	all vapor - choked at exit	40.10	11697	3.08
783	10.00	re-entrant	101	0.2763	all vapor - choked at exit	42.81	11828	3.11
783	7.00	flush	101	0.488	x > 0.92 - choked at exit	31.45	15348	4.04
783	7.41	flush	101	0.4458	all vapor - choked at exit	30.58	13633	3.59
783	7.50	flush	101	0.435	all vapor - choked at exit	30.68	13346	3.51
783	8.00	flush	101	0.3875	all vapor - choked at exit	32.29	12512	3.29
783	8.17	flush	101	0.374	all vapor - choked at exit	32.39	12114	3.19
783	9.00	flush	101	0.3252	all vapor - choked at exit	36.85	11984	**3.15**
783	9.30	flush	101	0.3131	all vapor - choked at exit	38.46	12042	3.17
783	9.50	flush	101	0.3055	all vapor - choked at exit	40.10	12251	3.22
745	7.16	re-entrant	101	0.4214	all vapor - choked at exit	29.32	12355	3.25
745	7.50	re-entrant	101	0.3879	all vapor - choked at exit	30.12	11684	3.07
745	8.00	re-entrant	101	0.3463	all vapor - choked at exit	31.68	10971	2.89
745	8.04	re-entrant	101	0.3433	all vapor - choked at exit	31.78	10910	2.87
745	8.50	re-entrant	101	0.3151	all vapor - choked at exit	34.12	10751	**2.83**
745	9.00	re-entrant	101	0.2922	all vapor - choked at exit	36.96	10800	2.84
745	9.50	re-entrant	101	0.275	all vapor - choked at exit	39.89	10970	2.89
745	10.00	re-entrant	101	0.2609	all vapor - choked at exit	42.30	11036	2.90
745	7.00	flush	101	0.4627	x > 0.93 choked at exit	30.32	14029	3.69
745	7.16	flush	101	0.4458	all vapor - choked at exit	29.32	13071	3.44
745	7.50	flush	101	0.4083	all vapor - choked at exit	30.12	12298	3.24
745	8.00	flush	101	0.3636	all vapor - choked at exit	31.68	11519	3.03
745	8.04	flush	101	0.3605	all vapor - choked at exit	31.78	11457	3.01
745	8.50	flush	101	0.3303	all vapor - choked at exit	34.12	11270	**2.97**
745	9.00	flush	101	0.3061	all vapor - choked at exit	36.96	11313	2.98
745	9.50	flush	101	0.2879	all vapor - choked at exit	39.89	11484	3.02
745	10.00	flush	101	0.2734	all vapor - choked at exit	42.30	11565	3.04

The points of minimum wall heat flux fall within the range of possible supercritical states, as is shown in Figure B-1.

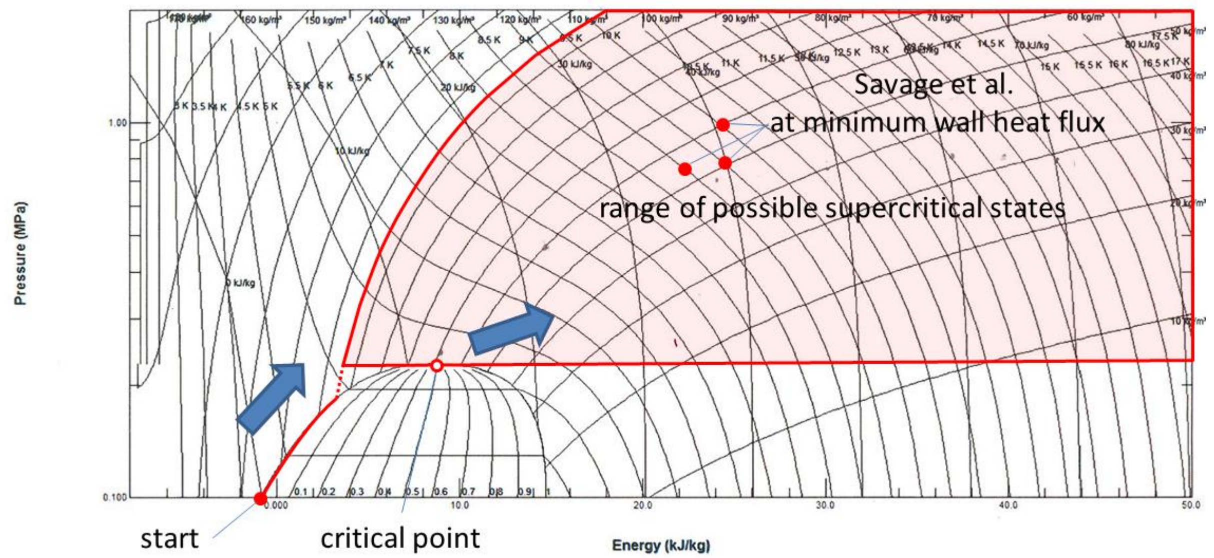

Figure B-1. Points of Minimum Wall Heat Flux in Savage et al.'s Experiments

The minimum calculated wall heat fluxes ranged from 2.83 to 3.45 W/cm^2. That is, at the peak supercritical pressure, the dewar heat load was *at least* 2.83 to 3.45 W/cm^2. These results are consistent with the recommended heat flux limit of 4 W/cm^2.

REPORT DOCUMENTATION PAGE	*Form Approved* *OMB No. 0704-0188*

The public reporting burden for this collection of information is estimated to average 1 hour per response, including the time for reviewing instructions, searching existing data sources, gathering and maintaining the data needed, and completing and reviewing the collection of information. Send comments regarding this burden estimate or any other aspect of this collection of information, including suggestions for reducing this burden, to Department of Defense, Washington Headquarters Services, Directorate for Information Operations and Reports (0704-0188), 1215 Jefferson Davis Highway, Suite 1204, Arlington, VA 22202-4302. Respondents should be aware that notwithstanding any other provision of law, no person shall be subject to any penalty for failing to comply with a collection of information if it does not display a currently valid OMB control number.
PLEASE DO NOT RETURN YOUR FORM TO THE ABOVE ADDRESS.

1. REPORT DATE *(DD-MM-YYYY)*	**2. REPORT TYPE**	**3. DATES COVERED** *(From - To)*
01- 10 - 2014	Technical Memorandum	August 2013 - August 2014

4. TITLE AND SUBTITLE
Maximum Expected Wall Heat Flux and Maximum Pressure after Sudden Loss of Vacuum Insulation on the Stratospheric Observatory for Infrared Astronomy (SOFIA) Liquid Helium (LHe) Dewars

5a. CONTRACT NUMBER

5b. GRANT NUMBER

5c. PROGRAM ELEMENT NUMBER

6. AUTHOR(S)
Ungar, Eugene K.

5d. PROJECT NUMBER

5e. TASK NUMBER

5f. WORK UNIT NUMBER
869021.03.07.01.01

7. PERFORMING ORGANIZATION NAME(S) AND ADDRESS(ES)
NASA Langley Research Center
Hampton, VA 23681-2199

8. PERFORMING ORGANIZATION REPORT NUMBER
L-20483 NESC-RP-13-00911

9. SPONSORING/MONITORING AGENCY NAME(S) AND ADDRESS(ES)
National Aeronautics and Space Administration
Washington, DC 20546-0001

10. SPONSOR/MONITOR'S ACRONYM(S)
NASA

11. SPONSOR/MONITOR'S REPORT NUMBER(S)
NASA/TM-2014-218540

12. DISTRIBUTION/AVAILABILITY STATEMENT
Unclassified - Unlimited
Subject Category 31 Engineering
Availability: NASA CASI (443) 757-5802

13. SUPPLEMENTARY NOTES

14. ABSTRACT
The aircraft-based Stratospheric Observatory for Infrared Astronomy (SOFIA) is a platform for multiple infrared observation experiments. The experiments carry sensors cooled to liquid helium (LHe) temperatures. A question arose regarding the heat input and peak pressure that would result from a sudden loss of the dewar vacuum insulation. Owing to concerns about the adequacy of dewar pressure relief in the event of a sudden loss of the dewar vacuum insulation, the SOFIA Program engaged the NASA Engineering and Safety Center (NESC). This report summarizes and assesses the experiments that have been performed to measure the heat flux into LHe dewars following a sudden vacuum insulation failure, describes the physical limits of heat input to the dewar, and provides an NESC recommendation for the wall heat flux that should be used to assess the sudden loss of vacuum insulation case. This report also assesses the methodology used by the SOFIA Program to predict the maximum pressure that would occur following a loss of vacuum event.

15. SUBJECT TERMS
NASA Engineering and Safety Center; Stratospheric Observatory for Infrared Astronomy; Field-Imaging Far-Infrared Line Spectrometer; Dewar; Wall Heat Flux

16. SECURITY CLASSIFICATION OF:			**17. LIMITATION OF ABSTRACT**	**18. NUMBER OF PAGES**	**19a. NAME OF RESPONSIBLE PERSON**
a. REPORT	**b. ABSTRACT**	**c. THIS PAGE**			STI Help Desk (email: help@sti.nasa.gov)
					19b. TELEPHONE NUMBER ***(Include area code)***
U	U	U	UU	45	(443) 757-5802

Standard Form 298 (Rev. 8-98)
Prescribed by ANSI Std. Z39.18